NIH Public Access
Author Manuscript
Gastroenterology. Author manuscript; available in PMC 2012 December 1.

Published in final edited form as:
Gastroenterology. 2011 December ; 141(6): 2200–2209. doi:10.1053/j.gastro.2011.08.008.

Accelerated and Progressive and Lethal Liver Fibrosis in Mice that Lack Interleukin (IL)-10, IL-12p40, and IL-13R α2

Margaret M. Mentink-Kane[1], **Allen W. Cheever**[2], **Mark S. Wilson**[1,§], **Satish K. Madala**[1,†], **Lara Megan Beers**[1], **Thirumalai R. Ramalingam**[1], and **Thomas A.Wynn**[1,*]

[1]Program in Barrier Immunity and Repair, Laboratory of Parasitic Diseases National Institute of Allergy and Infectious Diseases National Institutes of Health, Bethesda, Maryland 20892, USA

[2]Biomedical Research Institute, Rockville, MD 20852

Abstract

BACKGROUND & AIMS—Progressive fibrosis contributes to the morbidity of several chronic diseases; it typically develops slowly, so the mechanisms that control its progression and resolution have been difficult to model. The cytokines interleukin (IL)-10, IL-12p40, and IL-13Rα2 regulate hepatic fibrosis following infection with the helminth parasite *Schistosoma mansoni*. We examined whether these mediators interact to slow the progression of hepatic fibrosis in mice with schistosomiasis.

METHODS—*IL-10−/−*, *IL-12/23(p40)−/−*, and *IL-13Rα2−/−* mice were crossed to generate triple knockout mice (TKO). We studied these mice to determine whether the simultaneous deletion of these 3 negative regulators of the immune response accelerated mortality from liver fibrosis following infection with *S. mansoni*.

RESULTS—Induction of inflammation by *S. mansoni*, liver fibrosis, and mortality increased greatly in TKO mice, compared to wild-type mice; 100% of the TKO mice died by 10 weeks after infection. Morbidity and mortality were associated with the development of portal hypertension, hepatosplenomegaly, gastrointestinal bleeding, ascites, thrombocytopenia, esophageal and gastric varices, anemia, and increased levels of liver enzymes—all features of advanced liver disease. IL-10, IL-12p40, and IL-13Rα2 reduced the production and activity of the pro-fibrotic cytokine IL-13. A neutralizing antibody against IL-13 reduced the morbidity and mortality of the TKO mice following *S. mansoni* infection.

CONCLUSIONS—IL-10, IL-12p40, and IL-13Rα2 act cooperatively to suppress liver fibrosis in mice following infection with *S. mansoni*. This model rapidly reproduces many of the complications observed in patients with advanced cirrhosis, so it might be used to evaluate the efficacy of anti-fibrotic reagents being developed for schistosomiasis or other fibrotic diseases associated with a T-helper 2 cell-mediated immune response.

© 2011 The American Gastroenterological Association. Published by Elsevier Inc. All rights reserved

[*]**Corresponding Author:** To whom correspondence should be addressed: Dr. Thomas A. Wynn, Head: Immunopathogenesis Section, Laboratory of Parasitic Diseases, National Institute of Allergy and Infectious Diseases, National Institutes of Health, DHHS, 50 South Drive, Rm.6154, MSC 8003, Bethesda, MD 20892, 301-496-4758 (Telephone), twynn@niaid.nih.gov, 301-480-5025 (Fax).
[§]Current address: National Institute for Medical Research (NIMR), Molecular Immunology Division, Medical Research Council, London. NW7 1AA. UK
[†]Current address: Cincinnati Children's Hospital Medical Center, Pulmonary Medicine Cincinnati, OH 45229

Publisher's Disclaimer: This is a PDF file of an unedited manuscript that has been accepted for publication. As a service to our customers we are providing this early version of the manuscript. The manuscript will undergo copyediting, typesetting, and review of the resulting proof before it is published in its final citable form. Please note that during the production process errors may be discovered which could affect the content, and all legal disclaimers that apply to the journal pertain.

Conflict of Interest Statement: All of the authors acknowledge that no conflict of interest exists.

NIH-PA Author Manuscript
NIH-PA Author Manuscript
NIH-PA Author Manuscript

NIH-PA Author Manuscript

NIH-PA Author Manuscript

NIH-PA Author Manuscript

Keywords

Th2 response; mouse model; immune regulation; T-cell response; parasitic disease

INTRODUCTION

Liver fibrosis occurs in a variety of clinical settings and is typically associated with chronic disease including alcoholism, persistent or untreated infectious diseases (including viral hepatitis and schistosomiasis) and autoimmune hepatitis. Many cases of liver fibrosis in western societies are linked with non-alcoholic fatty liver disease (NAFLD) and associated with the rise in obesity and Type II diabetes[1]. Although the initiating stimuli vary, inflammation and fatty changes in the liver lead to hepatic cell damage and death. This in turn generates an immunological and tissue repair response. In chronic disease the tissue repair response results in excess collagen deposition and compromised liver function[2–4].

Immunoregulatory responses governing liver fibrosis have been modeled in mice infected with the parasitic helminth *Schistosoma mansoni*[5]. The parasite eggs become trapped in hepatic portal venules and induce granulomatous inflammation characterized by $CD4^+$ Th2 cells producing IL-4, IL-5 and IL-13[6]. The hepatic granulomas in turn elicit a tissue remodeling response including the induction of matrix metalloproteinases (MMPs), tissue inhibitors of metalloproteinases (TIMPs) and collagens[7]. In untreated human schistosomiasis, the repetitious cycle of tissue damage, inflammation and fibrosis can lead to severe life-threatening complications like portal hypertension, variceal bleeding and ultimately death, usually after several years of infection[8].

In addition to schistosome-induced liver fibrosis, other murine models have been developed to help identify factors that regulate liver fibrosis. These include carbon tetrachloride exposure, alcohol-induced fibrosis and bile-duct ligation (BDL)[9]. Although these models have provided many important insights on the initiation of fibrosis, they often fail to replicate the complications associated with chronic hepatic fibrosis, which include the development of portal hypertension, formation of esophageal varices, ascites, and anemia[10]. Development of these co-morbid conditions requires repeated injury to the liver and typically develops over a sustained period of time. Indeed, other than the chronic schistosome infection model, there are relatively few experimental models of fibrosis that generate the pathological sequelae associated with chronic and progressive disease. Because the primary goal of our research on liver fibrosis is to prevent or slow the development of these life-threatening sequelae[11], the murine model of schistosomiasis provides a useful system to evaluate the efficacy of anti-fibrotic therapies in a well-defined experimental model of chronic liver fibrosis[12].

Several studies have shown that the Th2-associated cytokine IL-13 serves as the principle driver of fibrosis following *S. mansoni* infection[13–15]. For example, mice deficient in IL-13 have reduced fibrosis compared to WT mice despite similar worm burdens and granulomatous inflammation. Consequently, *il13*$^{-/-}$ and *il-13Rα1*$^{-/-}$ mice survive infection much longer than their WT cohorts[15, 16]. We have been investigating the mechanisms that regulate IL-13 activity[17] and have identified three distinct negative regulatory pathways. These include IL-13Rα2 - a high affinity decoy receptor for IL-13[14]; IL-12p40 – a key driver of Th1 and Th17 responses[18], and IL-10 - a potent immunosuppressive cytokine[19]. Here, we intercrossed IL-13Rα2$^{-/-}$, IL-12/23(p40)$^{-/-}$ and IL-10$^{-/-}$ mice to generate a triple knockout mouse (TKO) and examined whether the progression to liver fibrosis was accelerated in the absence of three negative regulatory mechanisms.

NIH-PA Author Manuscript

NIH-PA Author Manuscript

NIH-PA Author Manuscript

MATERIALS AND METHODS

Mice

Female BALB/c, BALB/c IL-13Rα2$^{-/-}$, BALB/c IL-10$^{-/-}$, BALB/c IL-12/23(p40)$^{-/-}$, BALB/c IL-10$^{-/-}$IL-13Rα2$^{-/-}$, BALB/c IL-10$^{-/-}$IL-12/23(p40)$^{-/-}$, BALB/c IL-10$^{-/-}$ IL-12/23(p40)$^{-/-}$ IL-13Rα2$^{-/-}$ (all gene KO mice were backcrossed ≥10 generations to BALB/c), 6–8 weeks old were maintained at NIAID animal facilities at Taconic (Germantown, NY). All mice housed under specific pathogen-free conditions at the NIH in an AAALAC–approved facility in accordance with the procedures in the Guide for the Care and Use of Laboratory Animals under an animal study proposal approved by the NIAID Animal Care and Use Committee.

Infections and treatments

Mice were infected percutaneously via the tail with 25–35 cercariae of a Puerto Rican strain of *S. mansoni* (NMRI) (Biomedical Research Institute, Rockville, MD). Anti-IL-13 treatment was performed with rat anti-mouse IL-13 mAb (CNTO 134; IgG2a isotype, Centocor, Inc, Horsham, PA.)

RNA isolation, purification and real-time PCR

Total RNA was prepared from whole liver tissue samples as previously described[16]. Real-time polymerase chain reaction was performed on an ABI Prism 7900HT Sequence Detection System (Applied Biosystems). (Ramalingam, Pesce et al. 2008).

Histopathology and fibrosis

Tissues were fixed in Bouin-Hollande fixative and embedded in paraffin for sectioning and staining as described previously[16]. Liver collagens were measured as hydroxyproline after hydrolysis of 200 mg of liver in 5 ml of 6N HCl. The same individual scored all histological features and had no knowledge of the experimental design.

Hematology

EDTA-treated blood was processed at the NIH Clinical Center for automated counting using a Vista Analyzer (Siemens).

Occult fecal blood

Seracult Single Slide (Propper Mfg. Co., Inc. USA). Fecal pellets from individual mice were obtained at 8 wk pi and dispersed in saline using a Precellys 24 tissue homogenizer (Bertin Technologies). 0.10 mL of fecal specimen was applied to the slide and read for positive peroxidase activity within 60 seconds.

Intracellular cytokine staining

Leukocytes isolated from the livers of infected mice were stimulated for 3 h with phorbol 12-myristate13-acetate (10 ng/ml), ionomycin (1 mg/ml) and brefeldin A (10 mg/ml). Cell surfaces were stained with phycoerythrin–indodicarbocyanine–conjugated antibody to CD4 (anti-CD4; H129.19), were fixed for 20 min at 25 C in 2% (wt/vol) paraformaldehyde, were made permeable for 30 min with 0.1% saponin buffer and were further stained with fluorescein isothiocyanate–conjugated anti-IFN-γ (XMG1.2) phycoerythrin-conjugated anti-IL-13 (C531; Centocor), Alexa Fluor 647–conjugated anti-IL-4 (11B11) and allophycocyanin-conjugated anti-IL-5 (TRFK5) before being analyzed on a FACSCalibur (BD). Antibodies were from BD Pharmingen except where noted otherwise.

NIH-PA Author Manuscript

NIH-PA Author Manuscript

NIH-PA Author Manuscript

Statistics

All data were analyzed with GraphPad Prism (GraphPad Software; version 5) and statistical significance ($P<0.05$) was determined using a two-tailed unpaired student's t-test with a 95% confidence interval. Unless specified in the figure legends, all experiments and analyses were performed at least twice.

RESULTS

S. mansoni-induced inflammation, fibrosis, and mortality are increased in TKO mice

Mice infected with *S. mansoni* develop liver disease due to abundant egg deposition in the liver from long-lived worm pairs. Despite the heavy liver damage, *S. mansoni* infection in WT mice rarely causes death. This low mortality is attributed to host immunomodulatory mechanisms that regulate potentially harmful aspects of the immune response[12]. We were interested in examining the outcome of *S. mansoni* infection in mice for which specific downmodulatory mechanisms were genetically deleted. Groups of BALB/c mice and mice with targeted deletions of IL-10, IL-12/23(p40) and IL-13Rα2 (IL-10/IL-12/23(p40)/IL-13Rα2$^{-/-}$ designated "TKO") were exposed to 25–35 *S. mansoni* cercariae. As shown previously, BALB/c mice survived *S. mansoni* infection through wk 12 (Fig. 1A)[20]. In contrast, TKO mice displayed 100% mortality at acute infection. All TKO mice succumbed by week 10 pi, 3–4 weeks after the onset of egg deposition in the liver. We examined whether the mortality observed in TKO mice correlated with an increase in liver fibrosis. Groups of BALB/c and TKO mice were infected with *S. mansoni* and sacrificed on wk 8. Portions of liver were harvested to quantitate hydroxyproline levels (Fig. 1B) and granulomatous inflammation (Fig. 1C). Hydroxyproline levels in livers from naïve mice were not statistically different between the two age-matched groups (BALB/c 1.51 + 0.20 [mean + SD] and TKO 2.04 + 0.34[mean + SD] μmoles hydroxyproline /liver). As shown previously, inflammation and fibrosis is established in infected BALB/c by wk 8 pi, however fibrosis more than doubled in TKO mice and the granuloma volumes around newly deposited eggs were significantly increased. The extent of fibrosis was evident in picrosirius red-stained liver sections, where large deposits of collagen were observed around the granulomas and throughout the liver parenchyma in TKO mice (Fig. 1D). Similar studies conducted with a carbon tetrachloride exposure model of liver fibrosis did not produce similar results (Supplemental Fig. S1), suggesting that distinct mediators may be regulating fibrosis in each model.

Cytokine production by liver infiltrating CD4^{+} and CD4^{-} cells was assessed by *ex vivo* intracellular cytokine staining. For these studies, mice were euthanized at 7.5 wk pi and granuloma-associated lymphocytes were isolated from the liver. As expected, we found significant numbers of IL-4^{+}, IL-5^{+} and IL-13^{+} expressing CD4^{+} lymphocytes in infected BALB/c (Fig. 1E). However, a significantly larger population of CD4^{+} T cells expressing Th2 cytokines was observed in TKO mice. This was also accompanied by a decrease in IFN-γ-expressing cells, suggesting that accelerated disease in TKO mice resulted from a more polarized and exaggerated Th2-type response. IL-17A was not detectable (not shown).

Type-2 immunity is suppressed by three compensating regulatory mechanisms

Preliminary evidence from studies conducted with IL-10$^{-/-}$, IL-12p40$^{-/-}$ or IL-13Rα2$^{-/-}$ mice suggested that when a single regulatory gene was deleted, other suppressive mechanisms were increased to compensate for the missing pathway[20–22]. To investigate this further, we generated a panel of WT, single, double, and triple gene KO mice and compared the expression of IL-10, IL-13Rα2, and IFN-γ mRNA in granulomatous livers following infection with *S. mansoni*. Because the majority of TKO mice died by wk 9 pi, gene expression was evaluated in the liver by real-time qPCR between wk 7 and 8. Although

NIH-PA Author Manuscript

NIH-PA Author Manuscript

NIH-PA Author Manuscript

IL-10 mRNA expression is induced in the livers of BALB/c following infection, the IL-13Rα2$^{-/-}$, IL-12p40$^{-/-}$, and IL-12$^{-/-}$/IL-13Rα2$^{-/-}$ mice each displayed a much more marked increase in IL-10 (Fig. 2A). A similar pattern was observed for the IL-12-inducible cytokine IFN-γ, which showed enhanced induction in IL-10$^{-/-}$ and IL-10/IL-13Rα2 dbl KO mice (Fig. 2B) Likewise, the IL-13 decoy receptor in IL-10$^{-/-}$/IL-12$^{-/-}$ mice is 2-fold higher than expression in WT mice (Fig. 2C) This differential regulation of gene transcription emphasizes the potential compensatory roles for each gene during infection with *S. mansoni*. Consistent with their established roles in regulating Th2 effector function[20–22], the absence of either IL-10, IL-12p40 or IL-13Rα2 yielded enhanced expression of Relm-α (*Retnla*), a signature IL-13-responsive gene (Fig. 2D)[23]. However, double KO and TKO mice displayed the most significant increases in Relm-α expression following *S. mansoni* infection. The IFN-γ-inducible MIG/CXCL9 transcript was not induced in infected WT mice but was slightly enhanced in IL-13Rα2$^{-/-}$ and induced 30-fold in the absence of IL-10 (Fig. 2E). These results indicate that in the absence of one or two negative regulators the host utilizes additional negative regulators to control IL-13-mediated signaling. Finally, little change in TGF-β1 expression was observed in any group (Fig. 2F), confirming the lack of liver TGF-β1-induction during schistosomiasis[24].

IL-10, IL-12p40 and IL-13Rα2 collaborate to suppress the progression to lethal liver disease

A series of experiments with WT, single and compound gene KO mice allowed us to examine liver fibrosis and mortality for a given genotype. Although hydroxyproline assays revealed significant increases in fibrosis in all single and double KO mice (with the exception of IL-12p40$^{-/-}$ animals), TKO mice displayed a more than 4-fold increase ($p<0.003$ by Student's t-test) in hepatic fibrosis (hypro/g liver/10,000 eggs) when compared with similarly infected WT mice (Fig. 3A and Supplemental Figs. S2A and S2B). The degree of fibrosis also increased nearly 2-fold when compared with all of the double KO mice. We examined procollagen VI (*Col6a1*) expression in the liver since it is upregulated during schistosoma infection and shown to be regulated in part by IL-13 signalling[16]. Procollagen VI expression correlated with hydroxyproline levels and was induced almost 10-fold more in the livers of TKO mice compared to WT (Fig. 3B). We also examined a larger panel of fibrosis-related genes and observed significantly increased expression of pro Col I, pro Col III, Timp1, and Mmp12 mRNA expression in TKO versus WT BALB/c mice (Supplemental Fig. S3). Interestingly, mmp13, which has been hypothesized to inhibit liver fibrosis in schistosomiasis[25], was expressed at significantly decreased levels in the livers of the TKO mice (Fig. S3). Finally, survival studies indicated that although a majority of TKO mice succumb to infection within just a few weeks after the onset of parasite egg deposition in the liver, compensatory mechanisms in the double KO strains reduced mortality, leading to chronic infection (>10 wk pi) (Fig. 3C). Of the single KO strains, only IL-10$^{-/-}$ and IL-13Rα2$^{-/-}$ mice typically display increased mortality following *S. mansoni* infection, as previously shown[20]. Increased fibrosis and mortality in the TKO mice was not due to increased infection intensity (Table 1).

TKO mice develop signs of portal hypertension: anemia, thrombocytopenia and fecal occult blood

For many people living in endemic areas, chronic schistosomiasis causes significant liver fibrosis and portal hypertension that eventually leads to additional pathological sequelae including hepatosplenomegaly, anemia and ascites[8]. In severe cases portal hypertension results in portal-systemic collateral vessel formation. Rupture of these GI varices can result in massive internal bleeding, the main cause of death in *S. mansoni* infection[8]. We asked whether similar clinical features developed in the highly fibrotic TKO mice following infection. Whole blood was obtained from BALB/c and TKO mice 8 wk pi for a complete

NIH-PA Author Manuscript

NIH-PA Author Manuscript

NIH-PA Author Manuscript

blood count (CBC). RBCs and platelets as well as hemoglobin and hematocrit were all significantly reduced in infected TKO mice when compared with BALB/c (Fig. 4A). In contrast, the white blood cell (WBC) count was significantly higher in TKO mice. We also observed more pronounced esophageal varices (Fig. 4B) and enlarged mesenteric venules (not shown) in the TKO mice versus BALB/c upon post-mortem analysis and this condition was unique to *S. mansoni* infection since varices were not observed in naïve mice. Ascites was also found in approximately 50% of the TKO mice, while none was detectable in WT BALB/c mice at this early time point. Although splenomegaly was observed in both groups by wk 8 pi, a significant increase in spleen size was observed in TKO mice (Fig. 4C). In addition, TKO mice had elevated liver enzymes, particularly aspartate aminotransferase (AST) suggestive of increased hepatocyte damage and cell death (Fig 4D). Finally, since the TKO mice developed splenomegaly and severe anemia and rapidly succumbed to infection, we examined the stools of infected mice for occult blood at 6 and 8 wk pi as an indication of GI bleeding. At 8 wk pi, 100% of the TKO mice were fecal occult blood positive compared to 50% of WT mice (Fig. 4E). Post mortem analysis showed that GI bleeds were likely the primary cause of death.

TKO mice provide a rapid pre-clinical model to test novel anti-fibrotic drugs in schistosomiasis

Because patients diagnosed with hepatic fibrosis often already have many of the complications associated with advanced disease, a major goal for anti-fibrotic drug development is to slow disease progression and reduce morbidity and mortality. Since schistosome infected TKO mice rapidly developed many of the pathological sequelae associated with advanced liver fibrosis, they provide an ideal tool to test the efficacy of novel anti-fibrotic drugs in an accelerated model that more closely mirrors human schistosomiasis. We and others have previously shown that the development of liver fibrosis in schistosomiasis is IL-13-dependent. Liver fibrosis is significantly reduced in *il-13*$^{-/-}$ and *il-13Rα1*$^{-/-}$ mice[13, 15], as well as in WT mice treated with soluble IL-13Rα2-Fc which antagonizes IL-13 signaling[14]. Therefore we asked whether similar treatments with anti-IL-13 mAb could reduce severe fibrosis and downstream complications observed in infected TKO mice. For these experiments, BALB/c and TKO mice were infected with *S. mansoni* for 8 weeks. Beginning on wk 5 pi, groups of mice were treated with either anti-IL-13 Ab or control IgG once per week until wk 8[26]. Anti-IL-13 Ab treatment significantly reduced liver fibrosis in WT mice (Fig. 5A and Supplemetal Figs. S4A and S4B) and in addition, reduced the overwhelming liver fibrosis that developed in TKO mice. The reduction in liver fibrosis was also associated with a marked reduction in *Col6a* mRNA expression (Fig. 5B). Liver sections stained with picrosirius red and viewed under polarized light also revealed a reduction in collagen deposition in the anti-IL-13-treated TKO mice (Fig. 5C). Exacerbated hepatomegaly observed in infected TKO mice was also reversed by anti-IL-13 treatment (Fig. 5D) but did not change splenomegaly for either group (not shown). In addition, anti-IL-13 treatment reversed the anemic and thrombocytopenic status of infected TKO mice (Fig. 5E) and fewer anti-IL-13 treated TKO mice developed ascites (data not shown).

Since anti-IL-13 treatment succeeded in ameliorating liver fibrosis and normalized the CBCs of infected TKO mice, we performed a final series of experiments to determine whether a longer course of anti-IL-13 mAb could slow the progression to lethal disease. We also examined whether terminating therapy would provide sustained protection or allow the disease to progress. For these studies, a large group of TKO mice was infected with *S. mansoni* and separate groups were either left untreated or treated with isotype matched control IgG or anti-IL-13 starting on wk 6 and terminating on wk 14. As expected, untreated and control Ig-treated mice began dying during acute infection with the majority of mice succumbing by wk 9 (Fig. 6A). In marked contrast, less than 25% of the anti-IL-13 mAb

NIH-PA Author Manuscript

NIH-PA Author Manuscript

NIH-PA Author Manuscript

treated mice died during this period. Hardened, gray livers were observed in control IgG-treated and untreated mice but not in the anti-IL-13 treated group (Fig. 6B). Interestingly, even though the therapy was terminated on wk 14, 50% of the anti-IL-13 mAb-treated mice remained alive past wk 25 despite ongoing and similar infection intensities, suggesting that a relatively short course of anti-IL-13 mAb can provide sustained protection from lethal disease. Thus, blocking IL-13 was sufficient to reduce fibrosis, prevent anemia and thrombocytopenia and improve survival in mice susceptible to accelerated and severe hepatic fibrosis.

DISCUSSION

Fibrosis develops in a variety of human diseases including cirrhosis, macular degeneration, atherosclerosis, fatty acid liver disease and the pulmonary fibroses[27]. Modeling fibrogenesis and identifying mechanisms that regulate the progression of fibrosis are the focus of many *in vivo* studies[27]. Here we identified distinct but collaborating roles for IL-10, IL-12p40, and IL-13Rα2 in the suppression of hepatic fibrosis during infection with the helminth parasite *S. mansoni*. In the absence of all three key immunoregulatory factors, mice infected with *S. mansoni* developed rapidly accelerated liver fibrosis which contributed to the development of anemia, thrombocytopenia, gastrointestinal bleeding, ascites and mortality within 3 to 4 weeks after the onset of egg deposition in the liver. Strikingly, the pathological sequelae observed in TKO mice during acute infection mirrored the pathology that normally develops in chronically infected wild-type mice (> 36 weeks)[20], suggesting that this accelerated model of liver fibrosis may be used to more quickly and comprehensively evaluate the efficacy of experimental anti-fibrotic drugs, particularly those targeting the IL-13 pathway of fibrosis.

Immunoregulatory cytokines and their cognate receptors have been identified as host factors with the potential to exacerbate or inhibit the fibrotic process. The role of IL-10 in the development of fibrosis has been controversial, with some studies demonstrating a pro-fibrotic role for IL-10[28–30] and other studies identifying clear inhibitory roles[31–33]. On one hand, IL-10 is known to suppress pro-inflammatory chemokines and cytokines (MIG/CXCL9, TNF-α, IFN-γ, IL-12) that otherwise contribute to inflammation, tissue damage and ultimately the formation of fibrosis[34]. On the other hand, by inhibiting IL-12 and IFN-γ, two well known anti-fibrotic cytokines that normally inhibit collagen synthesis in fibroblasts[18, 35], IL-10 may indeed promote fibrosis. Thus, the cellular source (antigen-presenting cells, Th2 cells, $CD4^+CD25^+FoxP3^+$ T-regulatory cells), quantity, and pattern of expression of IL-10 likely influence whether IL-10 exhibits pro- or anti-fibrotic activity. Consistent with this hypothesis, we observed increased expression of IFN-γ in our *S. mansoni* infected IL-$10^{-/-}$ mice; however fibrosis was consistently increased in IL-10-deficient mice only when IL-12p40 was deleted simultaneously. These findings illustrate that IL-10 and the IFN-γ-inducing cytokine IL-12 interact collaboratively to inhibit the development of fibrosis[19].

In the combined absence of IL-10 and IL-12p40 schistosome-infected mice developed highly polarized and exaggerated Th2 responses. Because numerous studies have demonstrated that the Th2 cytokine IL-13 serves as the key driver of fibrosis in schistosomiasis[13–15, 24], the enhanced Th2 response in the IL-10/IL-12p40$^{-/-}$ mice likely explains why fibrosis increased. There are two distinct receptors that engage IL-13- the IL-4Rα/IL-13Rα1 heterodimer that serves as the primary stat6-activating receptor for IL-13- and IL-13Rα2, which functions as a high affinity decoy receptor for IL-13[16, 20]. Expression of the decoy receptor is induced on stromal cells e.g. fibroblasts, epithelium, and smooth muscle cells following stat6-activation[36–38]. Most studies have indicated that IL-13Rα2 primarily serves as an inducible antagonist of the IL-4Rα/IL-13Rα1 receptor complex[39, 40].

NIH-PA Author Manuscript

NIH-PA Author Manuscript

NIH-PA Author Manuscript

Interestingly, while development of Th2-driven fibrosis was augmented in IL-10$^{-/-}$/IL-12p40$^{-/-}$ mice, they also displayed marked increases in IL-13Rα2 expression, suggesting that the IL-13 decoy receptor was serving as an additional mechanism to control fibrosis in these mice. Indeed, comparison studies conducted with the various single, double, and triple knockout mice confirmed this hypothesis and demonstrated that IL-10, IL-12p40, and IL-13Rα2 were operating cooperatively to slow the progression of lethal hepatic fibrosis in schistosomiasis. Mechanistically, the immunosuppressive cytokine IL-10 and anti-fibrotic cytokine IL-12 inhibit fibrosis by reducing and antagonizing the production and profibrotic activity of IL-13, respectively, while IL-13Rα2 has an additional inhibitory effect by directly preventing IL-13 from engaging the signaling IL-4Rα/IL-13Rα1 complex. These findings nicely illustrate that when a single suppressive mediator is deleted, other negative regulatory pathways are augmented to compensate for the missing pathway. Thus, several compensatory mechanisms are involved in the regulation of lethal fibrotic disease.

It has been demonstrated previously that IL-4$^{-/-}$ and IL-4/10$^{-/-}$ mice are highly susceptible to *S. mansoni* infection[19, 41]. Like TKO mice, IL-4$^{-/-}$ and IL-4/IL-10$^{-/-}$ mice succumb to *S. mansoni* infection during acute infection. However, in contrast to TKO mice, IL-4$^{-/-}$ and IL-4/10$^{-/-}$ mice developed a completely different type of lethal pathology characterized by IFN-γ/TNF-α driven inflammation, large non-eosinophilic granulomas, an absence of significant hepatic fibrosis and sepsis due to intestinal damage[15, 19, 42]. Similar findings have also been reported in IL-4$^{-/-}$/IL-13$^{-/-}$ mice and in animals that develop Th1/Th17-dominant immune responses following *S. mansoni* infection[15, 43–45]. The common denominator in all of these mice is the absence of significant Th2 cytokine production, which results in an acutely lethal pro-inflammatory Th1/Th17-type immune response. Strikingly, TKO mice succumbed to *S. mansoni* infection in a similar time frame, with nearly 100% mortality observed by wk 10 post-infection. However, instead of developing an acutely lethal pro-inflammatory Th1/Th17-type response, the animals developed a highly exaggerated and acutely lethal pro-fibrotic immune response, characterized by enhanced IL-13 signaling and formation of many of the complications associated with cirrhosis.

Patients suffering from chronic and severe schistosomiasis often develop significant liver fibrosis (Symmer's pipestem fibrosis) that is complicated by secondary portal hypertension. Portal hypertension leads to the development of collateral vessels and porto-systemic shunting. The varices (tortuous and distended collateral veins) that form along the esophageal and rectal mucosa are associated with substantial risk of bleeding. Direct and indirect suppression of hematopoiesis along with increased blood loss in the gastrointestinal tract also contributes to the development of anemia. The results obtained with the TKO mouse suggest that the emergence of many of these complications in schistosomiasis is prevented or at least delayed significantly by the combined actions of IL-10, IL-12p40, and IL-13Rα2, which together inhibit both the production and activity of IL-13.

The critical role played by IL-13 was confirmed in a final series of experiments in which infected TKO mice were treated with a neutralizing monoclonal antibody against IL-13. In one study, four anti-IL-13 mAb treatments alone were successful in significantly reducing hepatic fibrosis. We also found that a longer course of treatment rescued the majority of infected mice from the development of severe morbidity and mortality. Indeed, the marked fibrosis, anemia, and hepatosplenomegaly observed in infected TKO mice returned to near WT levels following treatment with anti-IL-13.

In summary, by deleting key negative regulators of IL-13 effector function, we have developed a highly accelerated model of advanced liver fibrosis. As such, this novel mouse model highlights the important and overlapping levels of immunoregulation, which control the development of fibrosis. This model may serve as a useful tool to dissect the

NIH-PA Author Manuscript

NIH-PA Author Manuscript

NIH-PA Author Manuscript

mechanisms of Th2-driven fibrosis and provides an ideal approach to quickly evaluate the efficacy of novel anti-fibrotic drugs that target the IL-13 pathway of fibrosis.

Supplementary Material

Refer to Web version on PubMed Central for supplementary material.

Acknowledgments

The authors thank Sandy White, Anthony Tillory and additional staff in the NIAID animal facilities and Dr. Fred Lewis and colleagues (Biomedical Research Institute, Rockville, MD) for schistosome cercariae. We also thank our colleagues Luke Barron, Kevin Vannella, Kristen Kindrachuk and Robert Thompson (NIH) as well as Dr. Florian Rieder (Department of Gastroenterology & Hepatology, Digestive Disease Institute, Cleveland Clinic) for helpful discussions. Finally, we would like to thank Anuk Das and Patrick Branigan (Centocor, Inc.) for the anti-IL-13 mAb and Marion Kasaian and Mary Collins (Pfizer) for providing the original breeding pairs of IL-13Rα2$^{-/-}$ mice used in this study. This research was supported by the Intramural Research Program of the NIH, NIAID.

Mentink-Kane helped with study concept and design, acquisition of data, analysis and interpretation of data, and drafting of the manuscript. Cheever helped with data acquisition and analysis, interpretation of data, and statistical analysis. Wilson, Madala, Beers, and Ramalingam helped with study design, data acquisition, and critical revision of the manuscript. Wynn provided help with study concept and design, interpretation of data; drafting of the manuscript; critical revision of the manuscript, obtained funding, and provided study supervision.

Study funded by the intramural research program of NIAID/NIH

Abbreviations used

MMP	matrix metalloproteinase
CBC	complete blood count
WBC	white blood cell
WT	wild-type

REFERENCES

1. Starley BQ, Calcagno CJ, Harrison SA. Nonalcoholic fatty liver disease and hepatocellular carcinoma: a weighty connection. Hepatology. 2010; 51:1820–32. [PubMed: 20432259]
2. Bataller R, Brenner DA. Liver fibrosis. J Clin Invest. 2005; 115:209–18. [PubMed: 15690074]
3. Iredale JP. Models of liver fibrosis: exploring the dynamic nature of inflammation and repair in a solid organ. J Clin Invest. 2007; 117:539–48. [PubMed: 17332881]
4. Friedman SL. Mechanisms of hepatic fibrogenesis. Gastroenterology. 2008; 134:1655–69. [PubMed: 18471545]
5. Hoffmann KF, Wynn TA, Dunne DW. Cytokine-mediated host responses during schistosome infections; walking the fine line between immunological control and immunopathology. Adv Parasitol. 2002; 52:265–307. [PubMed: 12521263]
6. Pearce EJ, C MK, Sun J, J JT, McKee AS, Cervi L. Th2 response polarization during infection with the helminth parasite Schistosoma mansoni. Immunol Rev. 2004; 201:117–26. [PubMed: 15361236]
7. Vaillant B, Chiaramonte MG, Cheever AW, Soloway PD, Wynn TA. Regulation of hepatic fibrosis and extracellular matrix genes by the th response: new insight into the role of tissue inhibitors of matrix metalloproteinases. J Immunol. 2001; 167:7017–26. [PubMed: 11739522]
8. Cheever AW, Andrade ZA. Pathological lesions associated with Schistosoma mansoni infection in man. Trans R Soc Trop Med Hyg. 1967; 61:626–39. [PubMed: 4293432]
9. Hernandez-Gea V, Friedman SL. Pathogenesis of Liver Fibrosis. Annu Rev Pathol. 2010

NIH-PA Author Manuscript

NIH-PA Author Manuscript

NIH-PA Author Manuscript

10. Friedman SL. Seminars in medicine of the Beth Israel Hospital, Boston. The cellular basis of hepatic fibrosis. Mechanisms and treatment strategies. N Engl J Med. 1993; 328:1828–35. [PubMed: 8502273]
11. Iredale JP. Cirrhosis: new research provides a basis for rational and targeted treatments. BMJ. 2003; 327:143–7. [PubMed: 12869458]
12. Wilson MS, Mentink-Kane MM, Pesce JT, Ramalingam TR, Thompson R, Wynn TA. Immunopathology of schistosomiasis. Immunol Cell Biol. 2007; 85:148–54. [PubMed: 17160074]
13. Chiaramonte MG, Cheever AW, Malley JD, Donaldson DD, Wynn TA. Studies of murine schistosomiasis reveal interleukin-13 blockade as a treatment for established and progressive liver fibrosis. Hepatology. 2001; 34:273–82. [PubMed: 11481612]
14. Chiaramonte MG, Donaldson DD, Cheever AW, Wynn TA. An IL-13 inhibitor blocks the development of hepatic fibrosis during a T-helper type 2-dominated inflammatory response. J Clin Invest. 1999; 104:777–85. [PubMed: 10491413]
15. Fallon PG, Richardson EJ, McKenzie GJ, McKenzie AN. Schistosome infection of transgenic mice defines distinct and contrasting pathogenic roles for IL-4 and IL-13: IL-13 is a profibrotic agent. J Immunol. 2000; 164:2585–91. [PubMed: 10679097]
16. Ramalingam TR, Pesce JT, Sheikh F, Cheever AW, Mentink-Kane MM, Wilson MS, Stevens S, Valenzuela DM, Murphy AJ, Yancopoulos GD, Urban JF Jr. Donnelly RP, Wynn TA. Unique functions of the type II interleukin 4 receptor identified in mice lacking the interleukin 13 receptor alpha1 chain. Nat Immunol. 2008; 9:25–33. [PubMed: 18066066]
17. Wynn TA. IL-13 effector functions. Annu Rev Immunol. 2003; 21:425–56. [PubMed: 12615888]
18. Wynn TA, Cheever AW, Jankovic D, Poindexter RW, Caspar P, Lewis FA, Sher A. An IL-12-based vaccination method for preventing fibrosis induced by schistosome infection. Nature. 1995; 376:594–6. [PubMed: 7637808]
19. Hoffmann KF, Cheever AW, Wynn TA. IL-10 and the dangers of immune polarization: excessive type 1 and type 2 cytokine responses induce distinct forms of lethal immunopathology in murine schistosomiasis. J Immunol. 2000; 164:6406–16. [PubMed: 10843696]
20. Mentink-Kane MM, Cheever AW, Thompson RW, Hari DM, Kabatereine NB, Vennervald BJ, Ouma JH, Mwatha JK, Jones FM, Donaldson DD, Grusby MJ, Dunne DW, Wynn TA. IL-13 receptor alpha 2 down-modulates granulomatous inflammation and prolongs host survival in schistosomiasis. Proc Natl Acad Sci U S A. 2004; 101:586–90. [PubMed: 14699044]
21. Wynn TA, Eltoum I, Oswald IP, Cheever AW, Sher A. Endogenous interleukin 12 (Il-12) regulates granuloma formation induced by eggs of *Schistosoma mansoni* and exogenous IL-12 both inhibits and prophylactically immunizes against egg pathology. J Exp Med. 1994; 179:1551–1561. [PubMed: 7909326]
22. Wynn TA, Cheever AW, Williams ME, Hieny S, Caspar P, Kuhn R, Muller W, Sher A. IL-10 regulates liver pathology in acute murine Schistosomiasis mansoni but is not required for immune down-modulation of chronic disease. J Immunol. 1998; 160:4473–80. [PubMed: 9574553]
23. Loke P, Nair MG, Guiliano D, Parkinson J, Blaxter ML, Allen JE. IL-4 dependent alternatively-activated macrophages have a distinctive in vivo gene expression phenotype. Biomed Central. 2002; 3:7.
24. Kaviratne M, Hesse M, Leusink M, Cheever AW, Davies SJ, McKerrow JH, Wakefield LM, Letterio JJ, Wynn TA. IL-13 activates a mechanism of tissue fibrosis that is completely TGF-beta independent. J Immunol. 2004; 173:4020–9. [PubMed: 15356151]
25. Madala SK, Pesce JT, Ramalingam TR, Wilson MS, Minnicozzi S, Cheever AW, Thompson RW, Mentink-Kane MM, Wynn TA. MMP12-deficiency augments extracellular matrix degrading metalloproteinases and attenuates IL-13-dependent fibrosis. J Immunol. 2010 In Press.
26. Yang G, Volk A, Petley T, Emmell E, Giles-Komar J, Shang X, Li J, Das AM, Shealy D, Griswold DE, Li L. Anti-IL-13 monoclonal antibody inhibits airway hyperresponsiveness, inflammation and airway remodeling. Cytokine. 2004; 28:224–32. [PubMed: 15566951]
27. Wynn TA. Cellular and molecular mechanisms of fibrosis. J Pathol. 2008; 214:199–210. [PubMed: 18161745]

NIH-PA Author Manuscript

NIH-PA Author Manuscript

NIH-PA Author Manuscript

28. Barbarin V, Xing Z, Delos M, Lison D, Huaux F. Pulmonary overexpression of IL-10 augments lung fibrosis and Th2 responses induced by silica particles. Am J Physiol Lung Cell Mol Physiol. 2005; 288:L841–8. [PubMed: 15608148]
29. Lee CG, Homer RJ, Cohn L, Link H, Jung S, Craft JE, Graham BS, Johnson TR, Elias JA. Transgenic overexpression of interleukin (IL)-10 in the lung causes mucus metaplasia, tissue inflammation, and airway remodeling via IL-13-dependent and -independent pathways. J Biol Chem. 2002; 277:35466–74. [PubMed: 12107190]
30. Sun L, Louie MC, Vannella KM, Wilke CA, Levine AM, Moore BB, Shanley TP. New concepts of IL-10 induced lung fibrosis: fibrocyte recruitment and M2 activation in a CCL2/CCR2 axis. Am J Physiol Lung Cell Mol Physiol. 2010
31. Thompson K, Maltby J, Fallowfield J, McAulay M, Millward-Sadler H, Sheron N. Interleukin-10 expression and function in experimental murine liver inflammation and fibrosis. Hepatology. 1998; 28:1597–606. [PubMed: 9828224]
32. Nelson DR, Lauwers GY, Lau JY, Davis GL. Interleukin 10 treatment reduces fibrosis in patients with chronic hepatitis C: a pilot trial of interferon nonresponders. Gastroenterology. 2000; 118:655–60. [PubMed: 10734016]
33. Louis H, Van Laethem JL, Wu W, Quertinmont E, Degraef C, Van den Berg K, Demols A, Goldman M, Le Moine O, Geerts A, Deviere J. Interleukin-10 controls neutrophilic infiltration, hepatocyte proliferation, and liver fibrosis induced by carbon tetrachloride in mice. Hepatology. 1998; 28:1607–15. [PubMed: 9828225]
34. Moore KW, de Waal Malefyt R, Coffman RL, O'Garra A. Interleukin-10 and the interleukin-10 receptor. Annu Rev Immunol. 2001; 19:683–765. [PubMed: 11244051]
35. Granstein RD, Murphy GF, Margolis RJ, Byrne MH, Amento EP. Gamma-interferon inhibits collagen synthesis in vivo in the mouse. J Clin Invest. 1987; 79:1254–8. [PubMed: 3104404]
36. Lordan JL, Bucchieri F, Richter A, Konstantinidis A, Holloway JW, Thornber M, Puddicombe SM, Buchanan D, Wilson SJ, Djukanovic R, Holgate ST, Davies DE. Cooperative effects of Th2 cytokines and allergen on normal and asthmatic bronchial epithelial cells. J Immunol. 2002; 169:407–14. [PubMed: 12077271]
37. Andrews AL, Nasir T, Bucchieri F, Holloway JW, Holgate ST, Davies DE. IL-13 receptor alpha 2: a regulator of IL-13 and IL-4 signal transduction in primary human fibroblasts. J Allergy Clin Immunol. 2006; 118:858–65. [PubMed: 17030238]
38. Morimoto M, Zhao A, Madden KB, Dawson H, Finkelman FD, Mentink-Kane M, Urban JF Jr. Wynn TA, Shea-Donohue T. Functional importance of regional differences in localized gene expression of receptors for IL-13 in murine gut. J Immunol. 2006; 176:491–5. [PubMed: 16365442]
39. Chiaramonte MG, Mentink-Kane M, Jacobson BA, Cheever AW, Whitters MJ, Goad ME, Wong A, Collins M, Donaldson DD, Grusby MJ, Wynn TA. Regulation and function of the interleukin 13 receptor alpha 2 during a T helper cell type 2-dominant immune response. J Exp Med. 2003; 197:687–701. [PubMed: 12642601]
40. Wood N, Whitters MJ, Jacobson BA, Witek J, Sypek JP, Kasaian M, Eppihimer MJ, Unger M, Tanaka T, Goldman SJ, Collins M, Donaldson DD, Grusby MJ. Enhanced interleukin (IL)-13 responses in mice lacking IL-13 receptor alpha 2. J Exp Med. 2003; 197:703–9. [PubMed: 12642602]
41. Brunet LR, Finkelman FD, Cheever AW, Kopf MA, Pearce EJ. IL-4 protects against TNF-alpha-mediated cachexia and death during acute schistosomiasis. J Immunol. 1997; 159:777–85. [PubMed: 9218595]
42. Brunet LR, Beall M, Dunne DW, Pearce EJ. Nitric oxide and the Th2 response combine to prevent severe hepatic damage during Schistosoma mansoni infection. J Immunol. 1999; 163:4976–84. [PubMed: 10528202]
43. Rutitzky LI, Bazzone L, Shainheit MG, Joyce-Shaikh B, Cua DJ, Stadecker MJ. IL-23 is required for the development of severe egg-induced immunopathology in schistosomiasis and for lesional expression of IL-17. J Immunol. 2008; 180:2486–95. [PubMed: 18250458]
44. Rutitzky LI, Hernandez HJ, Yim YS, Ricklan DE, Finger E, Mohan C, Peter I, Wakeland EK, Stadecker MJ. Enhanced egg-induced immunopathology correlates with high IFN-gamma in

NIH-PA Author Manuscript

NIH-PA Author Manuscript

NIH-PA Author Manuscript

murine schistosomiasis: identification of two epistatic genetic intervals. J Immunol. 2005; 174:435–40. [PubMed: 15611268]

45. Rutitzky LI, Lopes da Rosa JR, Stadecker MJ. Severe CD4 T cell-mediated immunopathology in murine schistosomiasis is dependent on IL-12p40 and correlates with high levels of IL-17. J Immunol. 2005; 175:3920–6. [PubMed: 16148138]

NIH-PA Author Manuscript
NIH-PA Author Manuscript
NIH-PA Author Manuscript

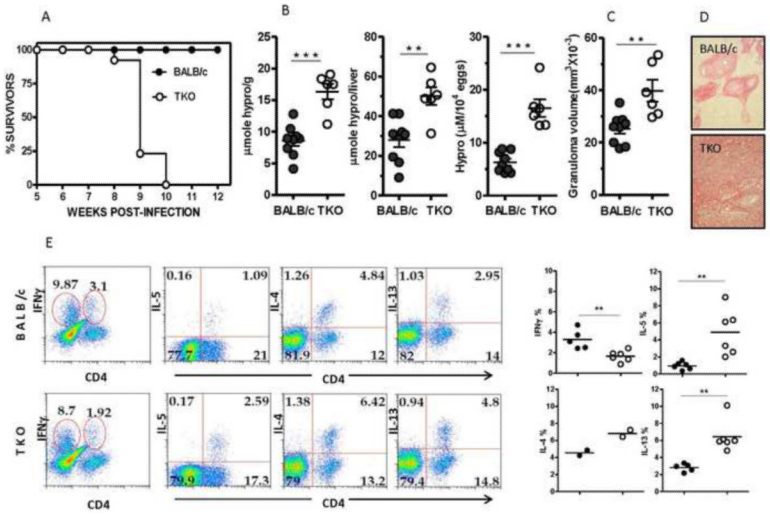

Figure 1. Increased fibrosis, inflammation, and mortality in TKO mice

(A) Survival of *S.mansoni* infected BALB/c (n=11) and TKO (n=13) mice, representative of 5 independent experiments. **(B)** Liver hydroxyproline content as μmoles/gram of liver tissue, μmoles/total liver and μmoles/10,000 *S. mansoni* eggs **(C)** granuloma size at 8 wk post-infection[13]. Each circle represents an individual mouse and bars the mean ± SEM. Data representative of 4 independent experiments. (**D**) Picrosirius red-stained paraffin-embedded liver sections at 8wk pi (**E**) Cytokine production by liver granuloma-associated CD4+ lymphocytesat 7.5wk pi.A representative analysis of two independent studies is shown. Scatter plot graphs depict CD4+ cytokine analysis (as in **E**) of two combined experiments with the horizontal bar showing the mean. Stars indicate significance in two-tailed Student's *t*-test; ***P*<0.005.

NIH-PA Author Manuscript
NIH-PA Author Manuscript
NIH-PA Author Manuscript

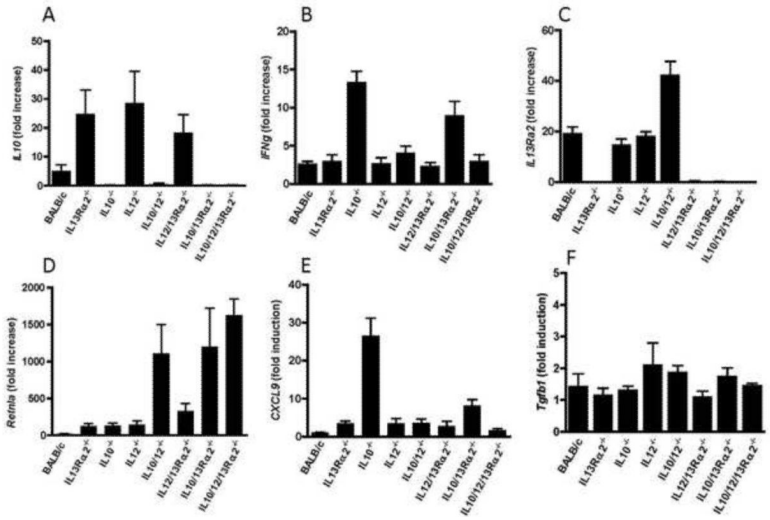

Figure 2. Compensatory expression of endogenous negative regulators in the liver

(**A**) Gene expression in the liver of BALB/c (N=9), IL-13α$^{-/-}$ (N=7), IL-10$^{-/-}$ (N=8), IL-12$^{-/-}$ (N=7), IL-10/IL-12(p40)$^{-/-}$ (N=8), IL-12(p40)/IL-13α2$^{-/-}$ (N=6), IL-10/IL-13Rα2$^{-/-}$ (N=7) and IL-10/IL-12(p40)/IL-13α2$^{-/-}$ (N=5) mice after 8wk infection with *S.mansoni*. Gene expression is normalized to HPRT and presented as the `fold increase' relative to expression in livers from naïve BALB/c mice. The analysis is representative of two independent experiments.

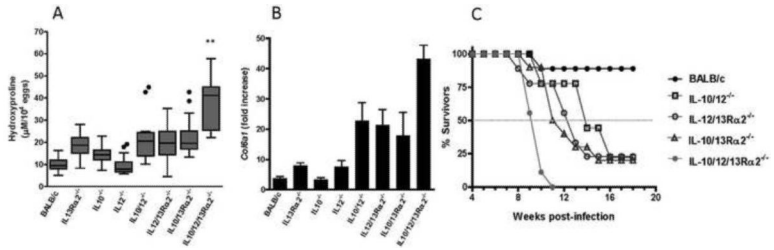

Figure 3. Exacerbated liver fibrosis in mice lacking one, two, or three endogenous regulators of IL-13

(A) The mice shown were infected with 35 cercariae of *S.mansoni* then sacrificed wk8 pi and fibrosis measured as liver hydroxyproline content. Because of variations in infection intensity between individual mice, the final hypro values were adjusted to take into account the number of *S. mansoni* eggs deposited in the liver. The reported hypro values are hypro/gram adjusted to 10,000 tissue eggs. Data combined from two independent experiments and expressed as box-and whisker plots with the horizontal line representing the median and whiskers extended to highest and lowest values with outliers shown at circels. (Outliers defined as lower than the 1st percentile and greater than the 99th percentile). Liver hydroxyproline values were significantly lower in all BALB/c WT, single, and double KO strains relative to TKO mice ($p \leq 0.003$ for all groups) (**B**) Liver *procollagen 6a1* mRNA levels at 8wk pi presented as the `fold increase' relative to expression in livers from naïve mice. (*, $p \leq 0.03$ for TKO mice compared to all seven control strains. (**C**) Survival following infection with 35 cercariae of *S.mansoni* (≥9 mice per group). TKO survival significantly accelerated relative to all 7 controls. Data are representative of 3 independent survival experiments (data for single KO mice not shown for figure clarity).

NIH-PA Author Manuscript NIH-PA Author Manuscript NIH-PA Author Manuscript

NIH-PA Author Manuscript
NIH-PA Author Manuscript
NIH-PA Author Manuscript

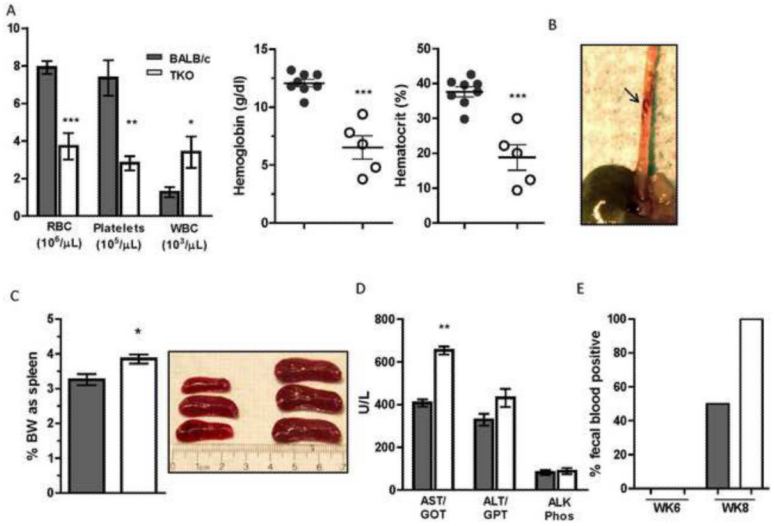

Figure 4. Anemia, thrombocytopenia and splenomegaly are exacerbated in infected TKO mice

(A) RBCs, platelets, WBCs, hemoglobin and hematocrit in the blood of 8wk *S.mansoni*-infected mice (n=5–8 mice per group). (**B**) Tortuous varix detected along the serosal surface of 8 wk infected TKO and engorged mesenteric venules are more prounounced in infected TKO mice (**C**) Splenomegaly depicted as % body weight (n=8 mice per group) and an image of three representative spleens shown from BALB/c and TKO mice. (**D**) Liver enzymes in serum at 8wk pi including: aspartate transaminase (AST), alanine transaminase (ALT) and alkaline phosphatase (ALK) (n ≥ 4 mice per assay) (**E**) Fecal occult blood detection at 6 and 8WK pi. *, $P \leq 0.02$, **, $P \leq 0.002$, ***, $P \leq 0.0002$.

NIH-PA Author Manuscript
NIH-PA Author Manuscript
NIH-PA Author Manuscript

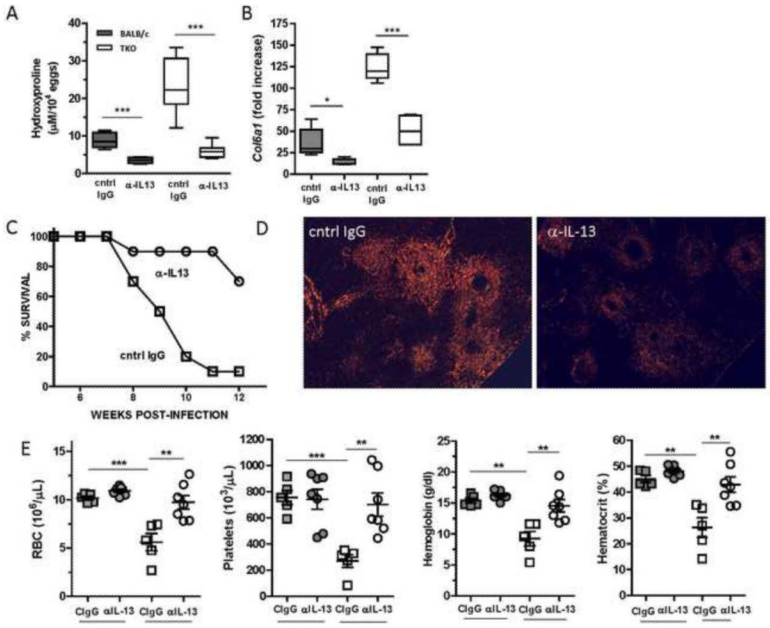

Figure 5. Blocking IL-13 inhibits liver fibrosis and reverses anemia following *S.mansoni* infection

(**A**) Mice infected with 35 cercariae of *S.mansoni* and between wk 5 and 8 treated with either rat-anti-mouse IL-13(IgG2a) or control (GL113) Ab at 0.5mg per mouse/week intraperitoneally (IP). Mice were sacrificed on wk8 pi and fibrosis measured as liver hydroxyproline (n= 6–9 mice per group). (**B**) Whole liver *procollagen 6a1* mRNA expression determined by real time PCR. (**C**) Survival of *S.mansoni* infected TKO treated with anti-IL-13 or cIgG. **(D)** Picrosirius red stained liver sections under polarized light on 5× magnification. (**E**) BALB/c and TKO mice infected then treated with control IgG or anti-IL-13 and heparinized blood was analyzed for RBCs, platelets, hemoglobin and hematocrit.

NIH-PA Author Manuscript

NIH-PA Author Manuscript

NIH-PA Author Manuscript

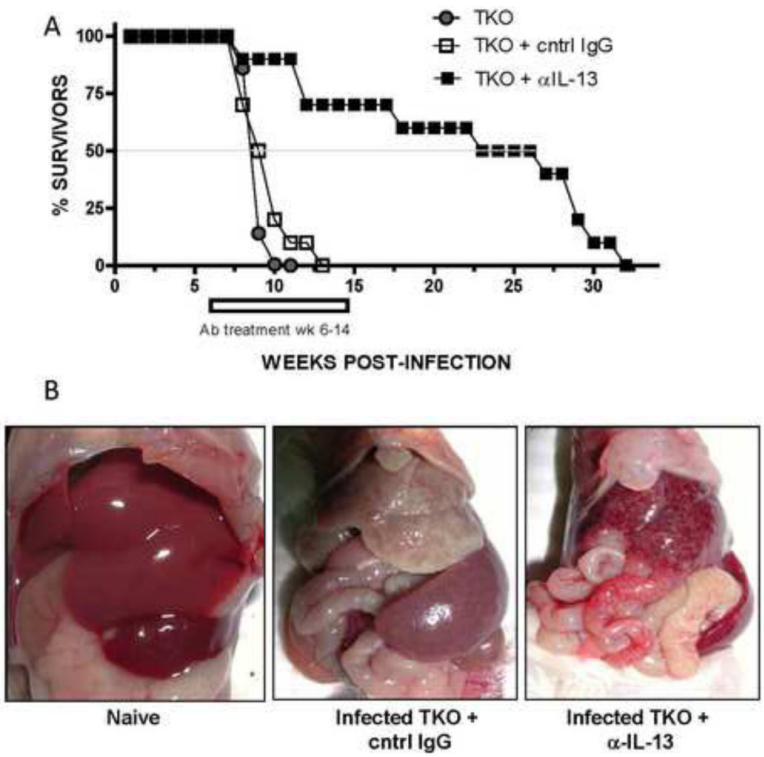

Figure 6. Anti-IL-13 treatment rescues TKO mice from death following *S.mansoni* infection

Thirty TKO mice were exposed to 25–35 cercariae of *S.mansoni*. From WK5 through WK12 pi, 10 of the mice were left untreated (closed circle); 10 mice received cntrl IgG (open square) and 10 mice received rat anti-IL-13 Ab (closed square). Ab treatment was administered I.P. at 0.5mg/mouse at 2×/week and survival monitored weekly. (**B**) Representative post-mortem images of TKO under naïve, control IgG- or anti-IL-13- treated conditions at 8wk pi.

NIH-PA Author Manuscript
NIH-PA Author Manuscript
NIH-PA Author Manuscript

Table 1

BALB/c, single KO, dbl KO and TKO mice were infected with 25–35 cercariae of *S.mansoni*. At 8wk, mice were sacrificed and perfused to quantitate (A) adult worm and (B) liver egg burden (number shown in 1000s). Mean ± SEM for two individual experiments is shown.

A	**BALB/c**	**IL13Rα2$^{-/-}$**	**IL10$^{-/-}$**	**IL12/23(p40)$^{-/-}$**	**IL10/12/33(p40)$^{-/-}$**	**IL12/23(p40)$^{-/-}$13Rα2$^{-/-}$**	**IL10/13Rα2$^{-/-}$**	**IL10/12/23(p40)13Rα2 $^{-/-}$**
Mean	2.94	3.07	3.38	2.73	2.69	2.47	2.50	1.54
SEM	0.29	0.31	0.55	0.25	0.38	0.35	0.37	0.21
B								
Mean	21.48	20.56	17.09	24.66	20.30	14.06	17.45	13.03
SEM	2.56	2.14	2.21	3.08	3.13	2.18	1.57	2.22